The influence of diverse substituents and their local interactions on linker rotational behaviors in MOFs by computational study

Shanghua Xing

2019. Jan. 17th

The 4th CREST Workshop

Flexible MOFs

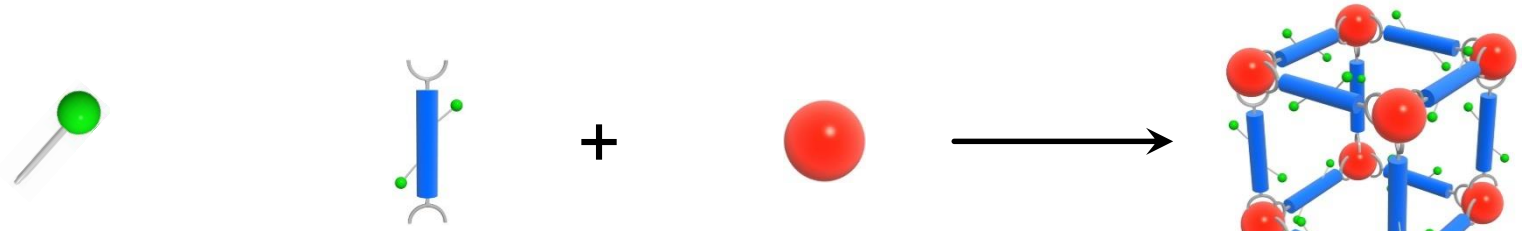

Substituent group (*eg*. NH_2, OCH_3 ..)

Ligand with substituent group

Metal ion (*eg*.Zn^{2+}, Cu^{+}..)

Functionalized MOF

❑ The flexibility on BDC linkers by different substituents[1,2]

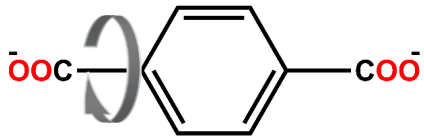

BDC linker

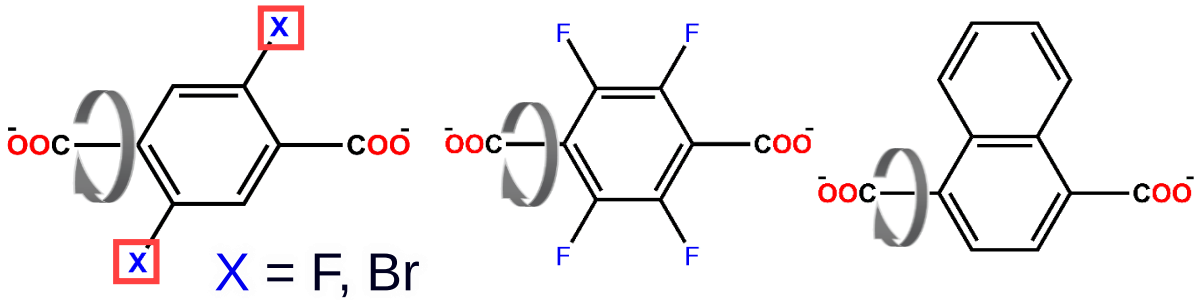

X = F, Br

BDC = 1,4-benzenedicarboxylates, X = substituent

Structural dynamics inside the functionalized MOFs

1. Matsuda. R. et al., Microporous Mesoporous Mater. **2014**, *189*, 83. 2. Damron J. et al., *Angew. Chem. Int. Ed.* **2018**, *57*, 8678.

PMMA

- Radical polymerization of Poly(methyl methacrylate) (PMMA) and its tacticity

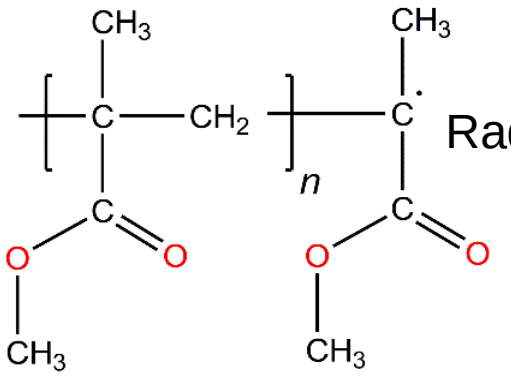

PMMA
radical terminal

Radical +

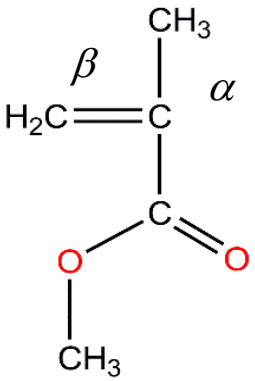

MMA (methyl methacrylate)
monomer

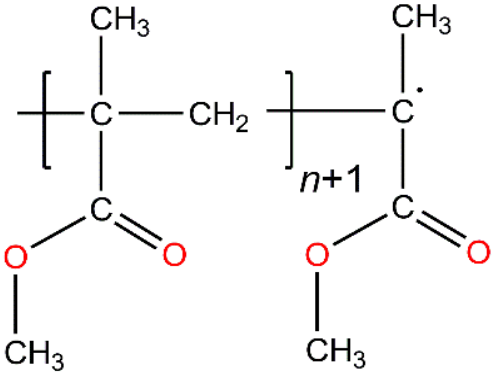

Elongated PMMA

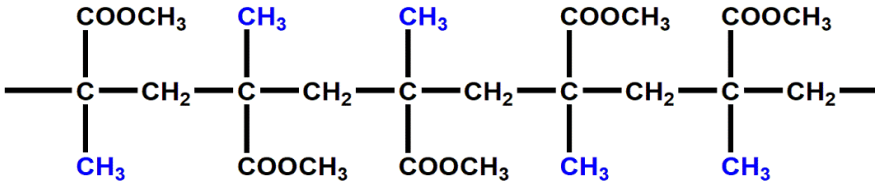

diad racemo meso r m
(r) (m)

triad rm mr rm

meso: two adjacent structure units in the same direction

racemo: two adjacent structure units in the opposite direction

Difficult tacticity control

Unique Tacticity Control

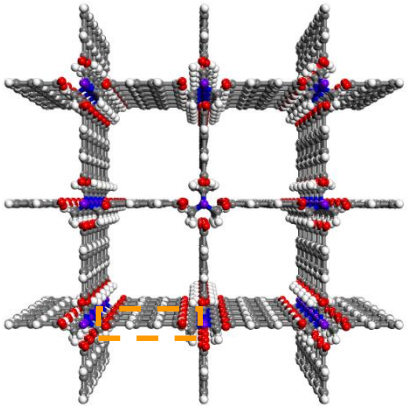

$[Zn_2(BDC\text{-}X)_2DABCO]_n$

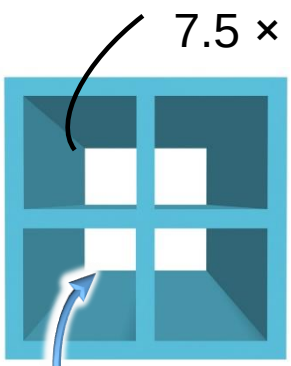

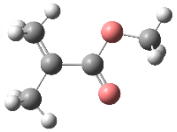

MMA monomer

MMA radical polymerization

within MOFs channel

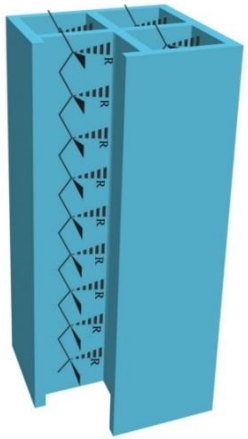

R= $COOCH_3$

Uemura, T. et al., *J. Am. Chem. Soc.* **2010**, *132*, 4917.

BDC-X	X	PMMA tacticity (%) mm:mr:rr (m)
Bulk polymerization		5:35:60 (22)
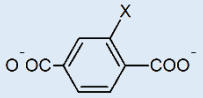	F	9:41:50 (30)
	OCH_3	13:44:43 (35)
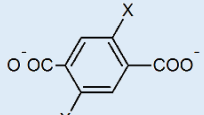	F	10:45:45 (32)
	OCH_3	28:53:19 (55)
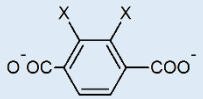	F	8:40:52 (28)
	OCH_3	8:39:53 (28)

meso ratio increase >30%

Tacticity control of MMA radical polymerization inside the functionalized MOFs

Research Plan

Experimental results reveal that BDC linker with different substituents (BDC-X) can realize the controllable tacticity of product PMMA polymerization. However, the atomistic mechanism of PMMA tacticity control by different substituents on polymerization is still under discussion.

The First Step

- ✓ To prepare the force field (FF) parameters for MOFs channel by the introduction of different substituents

The Second Step

- ✓ To investigate the tacticity dependency of PMMA on the organic linkers composing the MOF by using MD simulation

Model Preparation

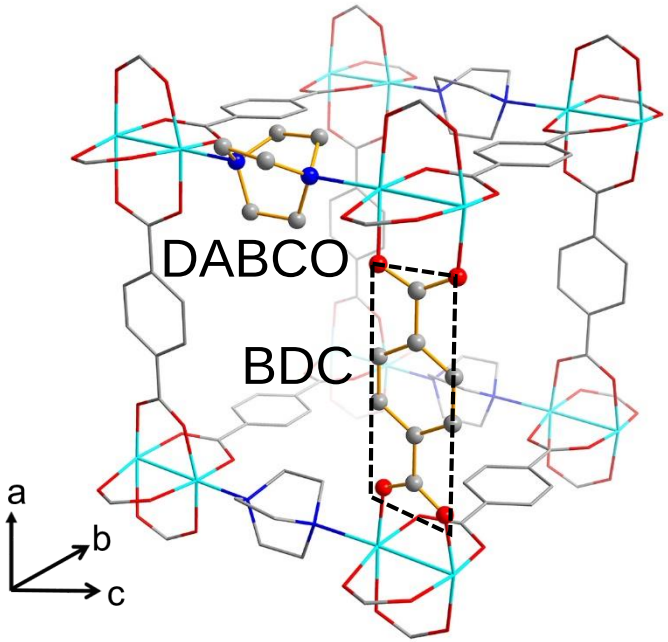

Simplified

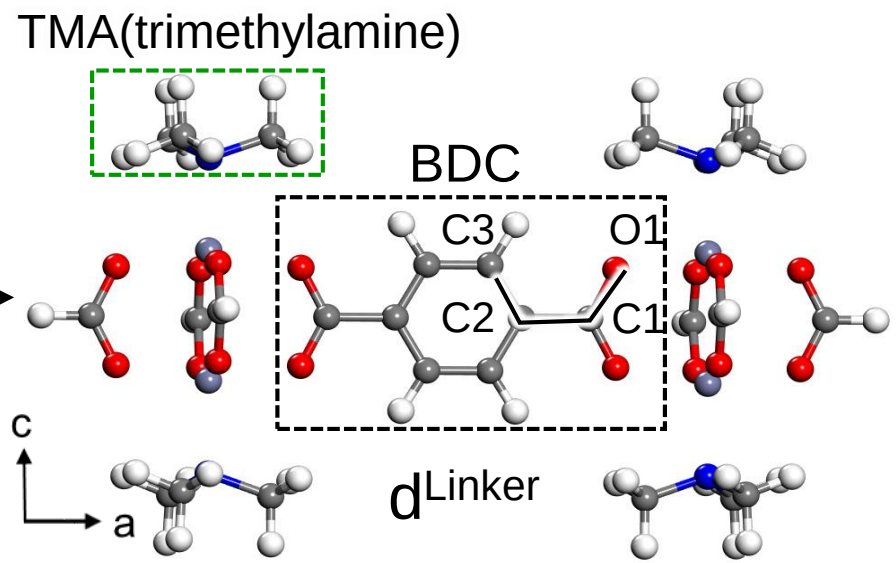

BDC Linker

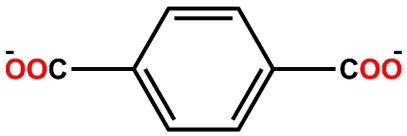

Non-substituent

BDC-X Linker

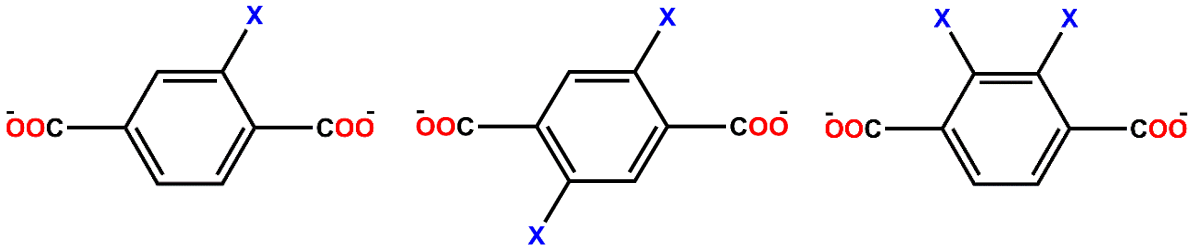

Mono-substituent 2,5-disubstituent 2,3-disubstituent

X = F, Cl, Br, NH_2, CH_3, OCH_3

Partial optimizations, Method: M06-2X/LANL2DZ (for Zn), 6-31G** (for other atoms)

Barrierless Rotation of DABCO

- The rotational behavior of DABCO linker

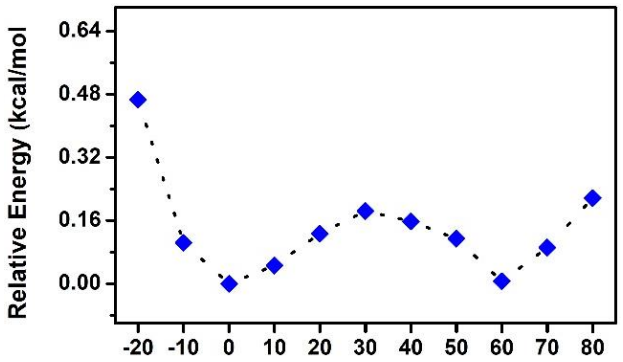

Two stable minima with 0° and 60°

Very low rotational barrier 0.18 kcal/mol at 30°

- DABCO model

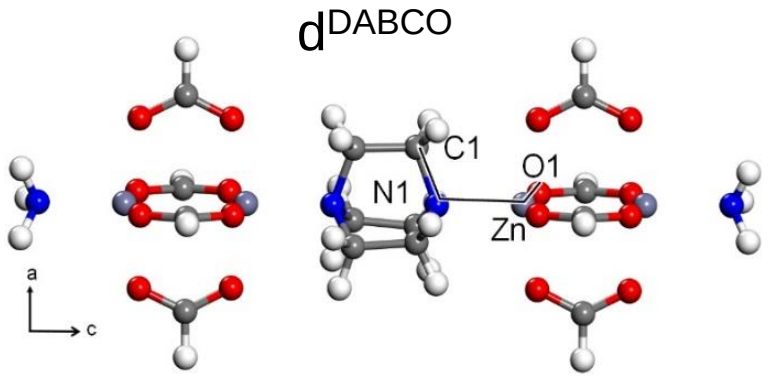

ΔE = 0.01 kcal/mol,

$E_{barrier}$ = 0.02 kcal/mol

- TMA model

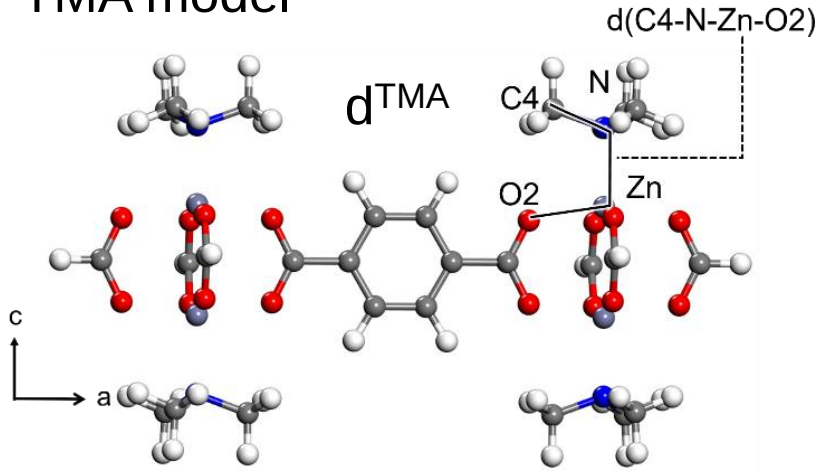

ΔE = 0.48 kcal/mol

$E_{barrier}$ = 0.71 kcal/mol

ΔE is the relative energy between 0 and 60°

All the calculations were performed by fixed four caps of d^{TMA} with 0°, 30° and 60°

Substituent-dependent Planarity

The equilibrium d^{Linker} in the most stable conformations for TMA model system

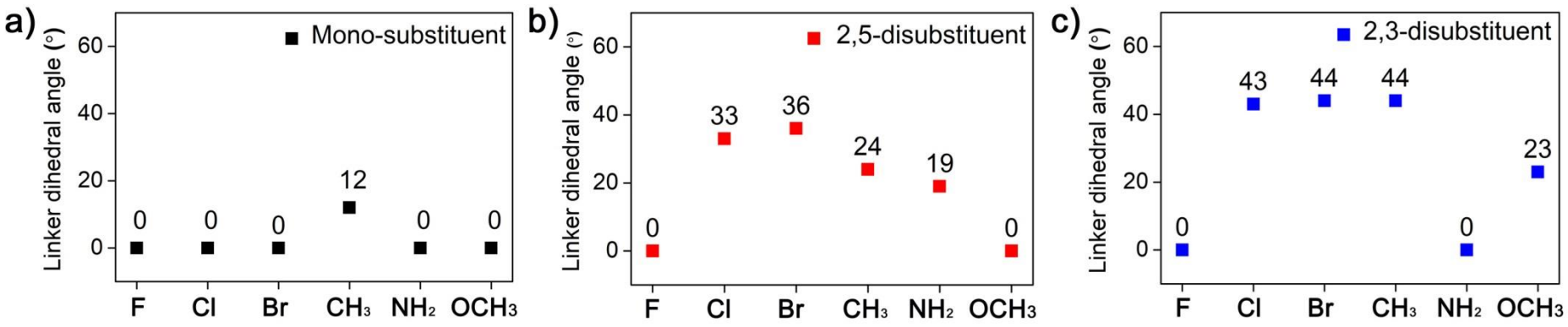

Finding in halogen substituent (-F, -Cl, -Br)

- ✓ F models are planar ($d^{Linker} = 0^{o}$) structures, but Cl and Br models are nonplanar.
- ✓ The d^{Linker} angle increase in the order of F < Cl < Br.

Finding in bulky substituents (-CH_3, -NH_2, -OCH_3)

- ✓ CH_3 models are the nonplanar structures, NH_2 models prefer the planar structures.
- ✓ OCH_3 models with mono- and 2,5-disubstituents are planar structures, but that with 2,3-disubstituent is nonplanar structure.

Diverse Rotational Barriers

The diverse rotational barriers at 90° (left) and 0° (right) in the most stable conformations.

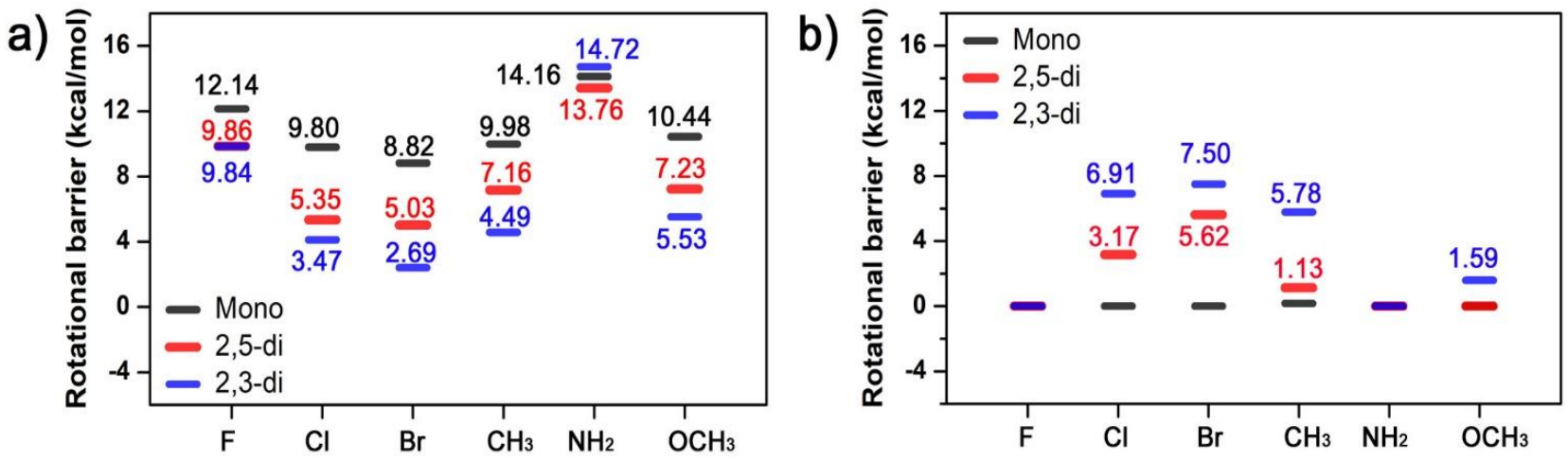

Finding in barriers at 90°

- ✓ The barriers in halogen substituent decrease in the order of F > Cl > Br.
- ✓ NH_2 substituents have the highest barrier.
- ✓ The barriers for OCH_3 models are higher than Cl, Br and CH_3 models.

Finding in barriers at 0°

- ✓ the barriers in 2,3-di are higher than 2,5-disubstituent.

TMA Rotational Effect

The most stable conformation considerably depends on the d^{TMA}

- *Example in 2,3-disubstituent with F, Cl and Br*

$d^{TMA} = 0°$
$d^{Linker} = 0°$, $r_{(F-H)} = 2.81$ Å
0.00 kcal/mol

$d^{TMA} = 0°$
$d^{Linker} = 46°$, $r_{(Cl-H)} = 3.05$ Å
0.00 kcal/mol

$d^{TMA} = 0°$
$d^{Linker} = 50°$, $r_{(Br-H)} = 3.13$ Å
0.00 kcal/mol

$d^{TMA} = 30°$
$d^{Linker} = 12°$, $r_{(F-H)} = 2.59$ Å
0.21 kcal/mol

$d^{TMA} = 30°$
$d^{Linker} = 41°$, $r_{(Cl-H)} = 3.23$ Å
-0.28 kcal/mol

$d^{TMA} = 30°$
$d^{Linker} = 44°$, $r_{(Br-H)} = 3.31$ Å
-0.15 kcal/mol

$d^{TMA} = 60°$
$d^{Linker} = 0°$

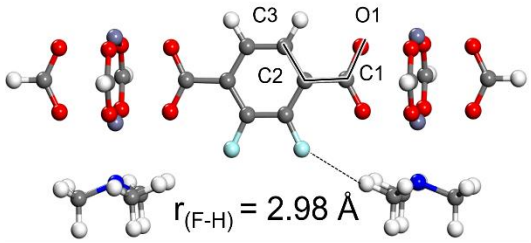

0.13 kcal/mol

$d^{TMA} = 60°$
$d^{Linker} = 0°$

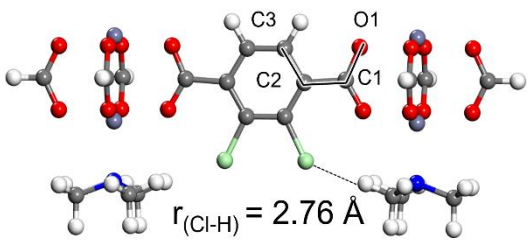

3.23 kcal/mol

$d^{TMA} = 60°$
$d^{Linker} = 0°$

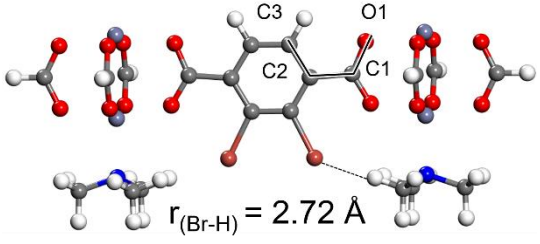

6.46 kcal/mol

The local interaction between the substituents and TMA cap is existed

Atomistic Mechanism of Planarity

Finding 1: F models are the planar structures, but Cl and Br models prefer the nonplanar

MOF_BDC with TMA cap		d^{TMA} (deg.)	Equilibrium *X*-H distance (Å)	d^{Linker} (deg.)
No substituent		0	2.97	0
F	Mono-	0	2.82	0
	2,5-di	0	2.85	0
	2,3-di	0	2.81	0
Cl	Mono-	60	2.87	0
	2,5-di	30	2.96	33
	2,3-di	30	3.23	43
Br	Mono-	60	2.86	0
	2,5-di	30	3.05	36
	2,3-di	30	3.31	44

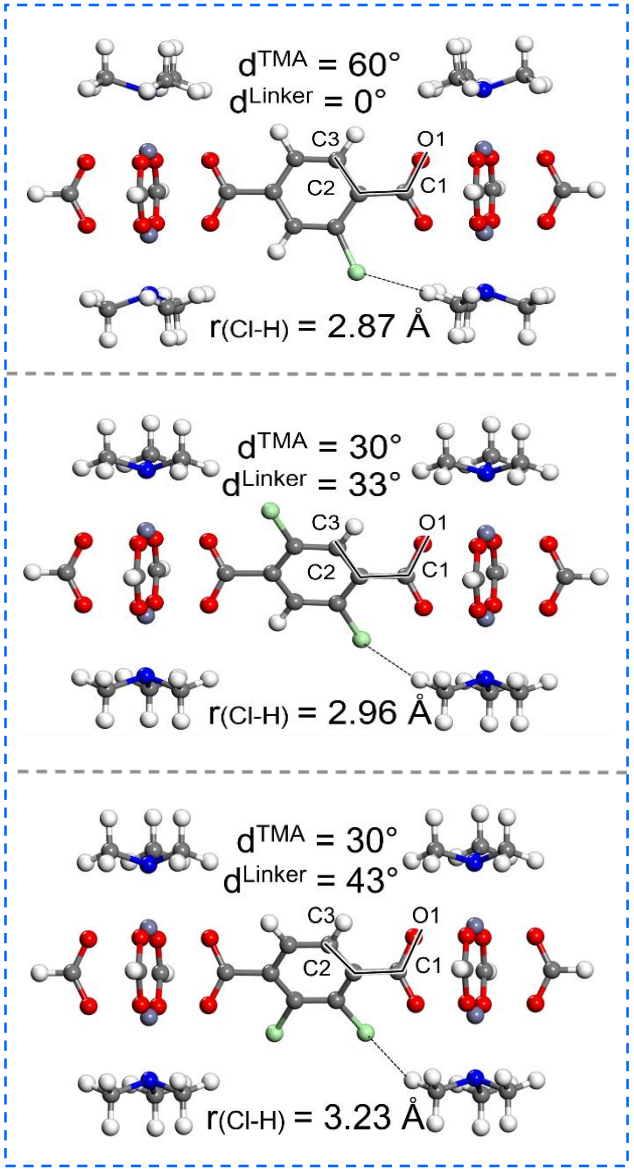

The sum of *vdW* radius in GAFF:
R(F-H) = 3.14 Å, R(Cl-H) = 3.34Å, R(Br-H) = 3.41Å

The equilibrium r(X-H) are shorter than the sum of vdW radius, indicating the presence of vdW repulsion

Atomistic Mechanism of Planarity

Finding 2: The d^{Linker} angle increase in the order of F < Cl < Br.

MOF_BDC with TMA cap		d^{TMA} (deg.)	d^{Linker} (deg.)	ChelpG charge *X*	ChelpG charge H
No substituent		0	0	0.0959	0.0775
F	Mono-	0	0	-0.1945	0.0781
	2,5-di	0	0	-0.1832	0.0793
	2,3-di	0	0	-0.1500	0.0804
Cl	Mono-	60	0	-0.1641	0.0865
	2,5-di	30	33	-0.1403	0.0885
	2,3-di	30	43	-0.1167	0.0907
Br	Mono-	60	0	-0.1092	0.0871
	2,5-di	30	36	-0.0948	0.0879
	2,3-di	30	44	-0.0800	0.0921

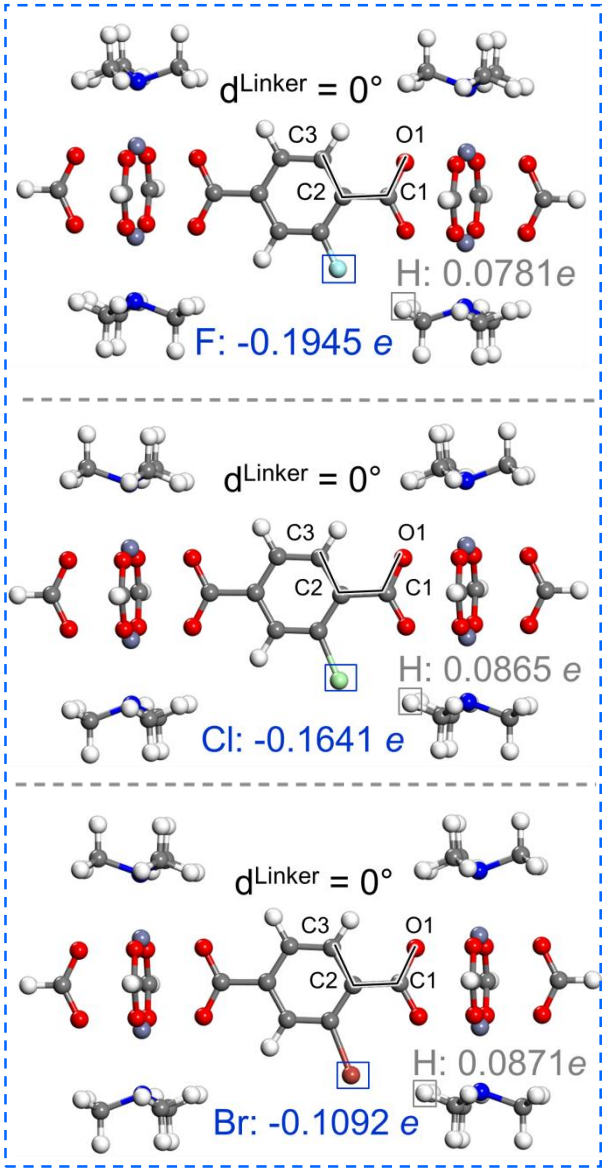

The strength of the electrostatic attraction is in the order of F > Cl > Br.

This partially contribute to the stability of the planar conformations of the F-substituents.

Atomistic Mechanism of Planarity

Finding 1: CH_3 models prefer the nonplanar, NH_2 models prefer the planar

MOF_BDC with TMA cap		d^{TMA} (deg.)	Equilibrium *X*-H distance (Å)	d^{Linker} (deg.)
No substituent		0	2.97	0
NH_2	Mono-	0	2.13	0
	2,5-di	30	2.17	19
	2,3-di	0	2.14	0
CH_3	Mono-	60	2.35	12
	2,5-di	60	2.31	24
	2,3-di	30	2.90	43

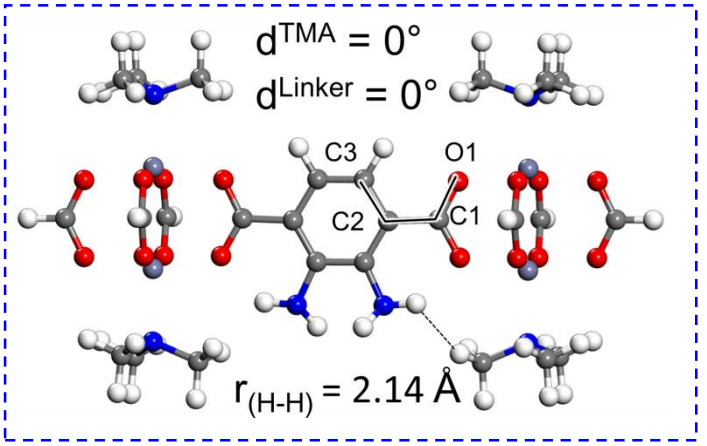

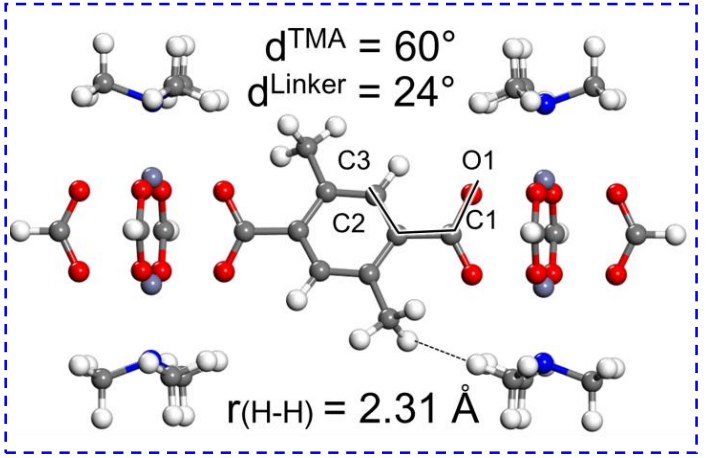

vdW repulsion affect the resulting nonplanar conformarion in CH_3 model

Small vdW repulsion result in the planar structures in NH_2 model

The sum of *vdW* radius in GAFF:
R(H-H) = 2.77 Å in CH_3, R(H-H) = 1.99 Å in NH_2

Atomistic Mechanism of Planarity

Finding 2: OCH_3 models with mono- and 2,5-disubstituents are planar structures, and that with 2,3-disubstituent is nonplanar structure.

MOF_BDC with TMA cap		d^{TMA} (deg.)	ΔE (kcal/mol)	Equilibrium *X*-H distance (Å)	d^{Linker} (deg.)	ChelpG charge *X*	ChelpG charge H
OCH_3	Mono-	0	0.00	2.73	0	-0.3078	0.0799
	2,5-di	0	0.00	2.76	0	-0.2839	0.0826
	2,3-di	60	-1.19	2.80	23	-0.3106	0.0845

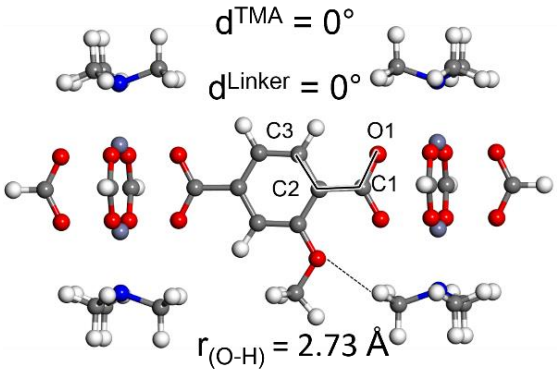

H bonding (CH…O)

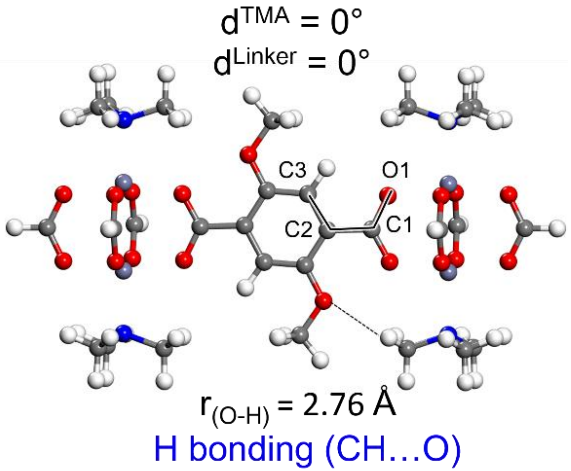

H bonding (CH…O)

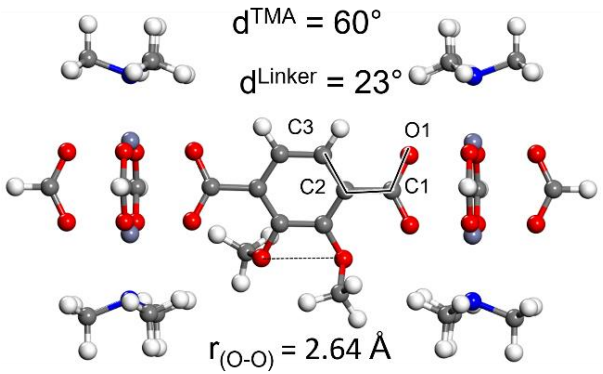

vdW repulsion

The sum of *vdW* radius in GAFF: R(O-O) = 3.37 Å

Atomistic Mechanism of Rotational Barriers

Finding 1: The barriers in halogen substituent decrease in the order of F > Cl > Br.

- Example in 2,5-disubstituent with F, Cl and Br

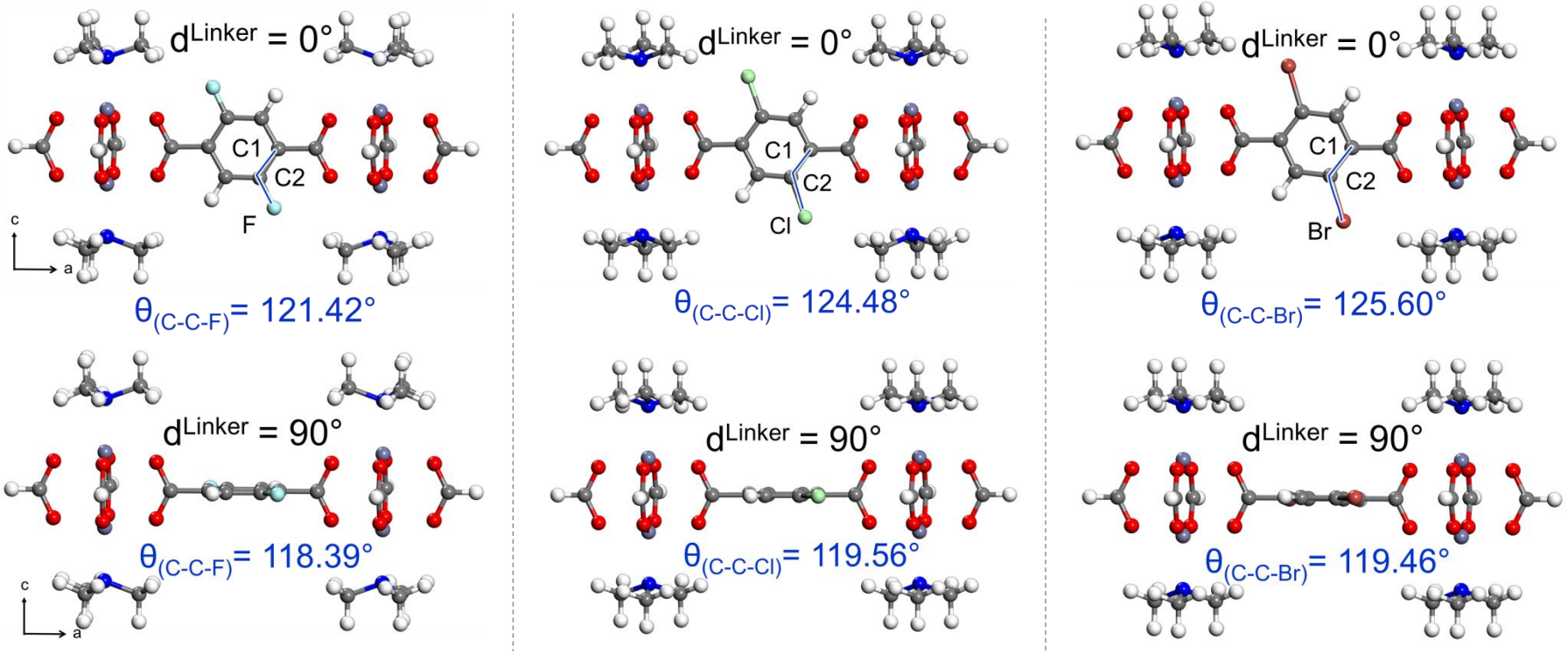

The increasing vdW repulsion of Br > Cl > F can be reflected by strain of $\theta_{(C\text{-}C\text{-}X)}$.
The θ angles at d^{Linker} = 90° are close to the angle $\theta_{(C\text{-}C\text{-}H)}$ = 118.57° in non-substituted model.

The destabilization of the conformations are in the order of Br > Cl > F, resulting in the observed rotational barrier order F > Cl > Br.

Atomistic Mechanism of Rotational Barriers

Finding 2: the barriers at 0° in 2,3-di are higher than 2,5-disubstituent.

- Example in 2,3-disubstituent with Br

Energy minimum

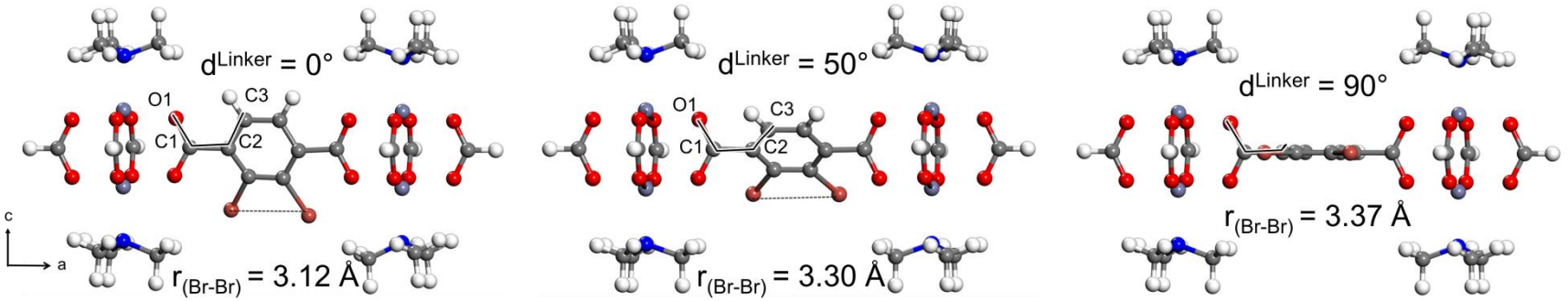

The strong strain at d^{linker} = 0° resulted in the higher rotational barriers at 0°.

The sum of *vdW* radius in GAFF: R(Br-Br) = 4.04 Å

Finding 3: NH_2 model among the substituent has the highest rotational barriers at 90°.

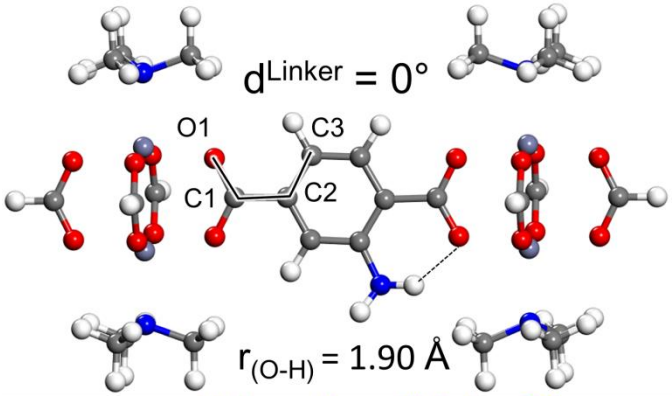

H bonding (NH…O)

At d^{linker} = 0°, NH_2 group interact with the carboxylate via H bonding (NH…O) that must be broken upon the rotation.

Atomistic Mechanism of Rotational Barriers

Finding 4: The barriers for OCH_3 models are higher than Cl, Br and CH_3 models.

- Example in mono-substituent with Cl, Br, CH_3 and OCH_3

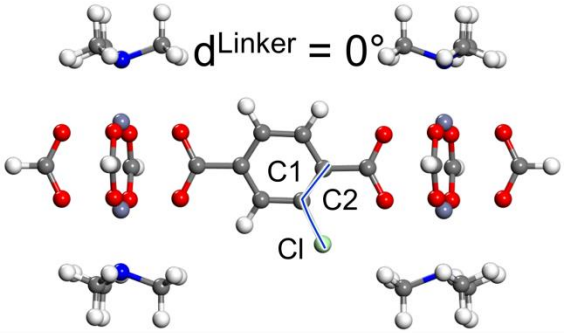

$\theta_{(C\text{-}C\text{-}Cl)}$= 123.92°

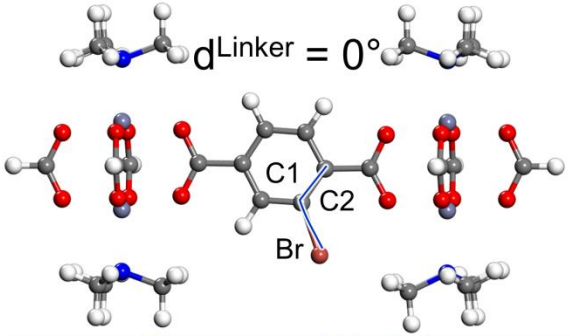

$\theta_{(C\text{-}C\text{-}Br)}$= 123.77°

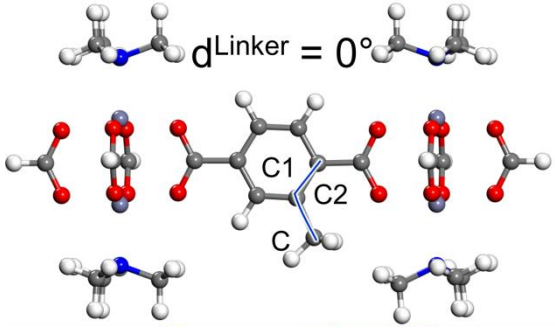

$\theta_{(C\text{-}C\text{-}C)}$= 124.49°

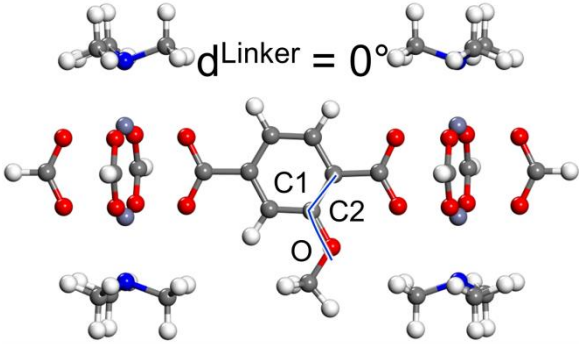

$\theta_{(C\text{-}C\text{-}O)}$= 119.21°

Cl, Br and CH_3 substituted models at $d^{linker} = 0^o$ are destabilized by the presence of vdW repulsion,

OCH_3-substituted model at $d^{linker} = 0^o$ is stabilized due to the presence of H bonding.

Only the angle θ in OCH_3 substituent is close to θ (C-C-H) in non-substituted model (118.57°)

FF Fitting of MOF channel

44 DFT conformations used for MM optimization

4 optimized structures by rotating d^{TMA} at 0, 60, e30 and s30 degree
4 partially relaxed scan structures with 10 degree interval for 10 times by keeping d^{TMA} at 0, 60, e30 and s30 degree.

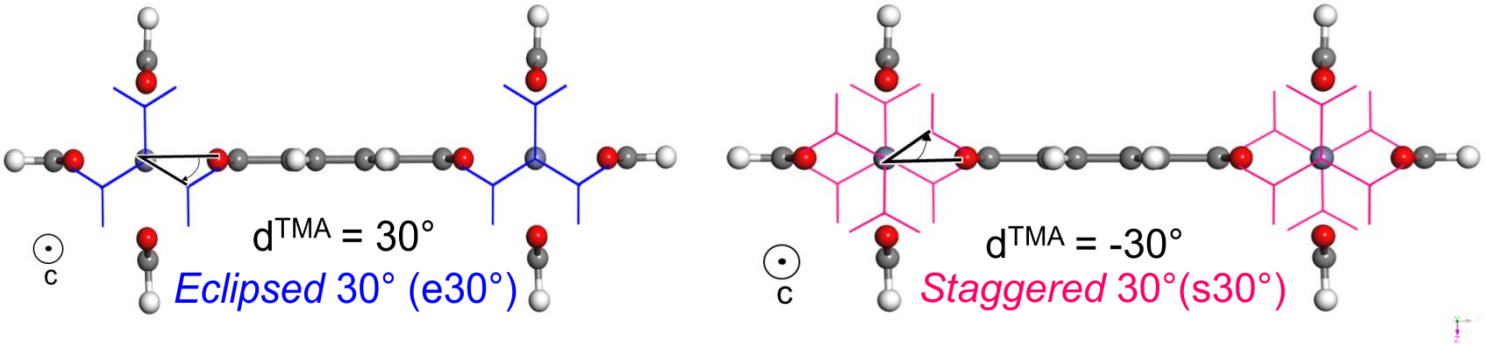

- *Example in 2,3-disubstituent with Br*

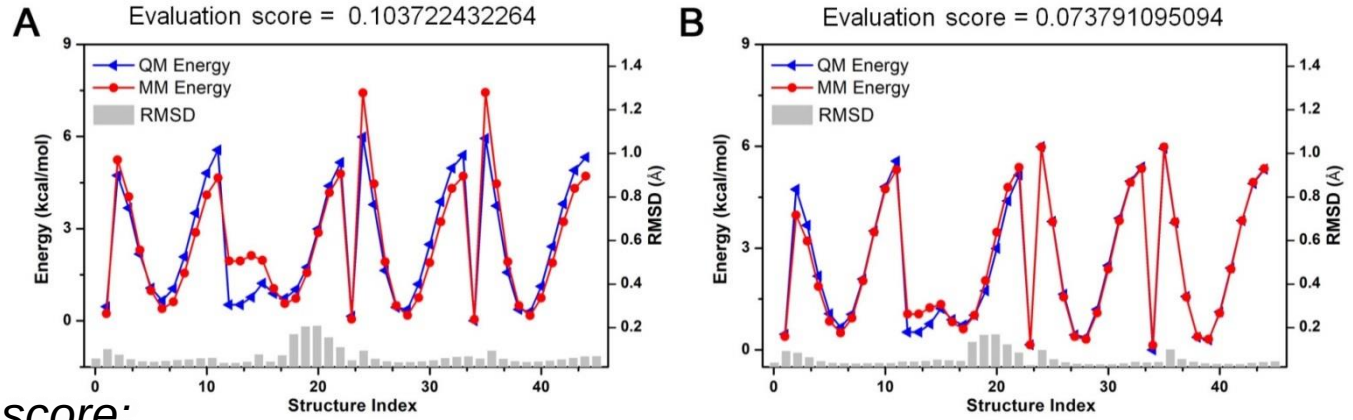

Evaluation score:

$$Score = weightE \times \frac{1}{n}\sum_{i=1}^{n}\left|\left(E_{\mathrm{mm}}^{(i)} - \overline{E_{\mathrm{mm}}}\right) - \left(E_{\mathrm{qm}}^{(i)} - \overline{E_{\mathrm{qm}}}\right)\right| + weightRMSD \times \frac{1}{n}\sum_{i=1}^{n} RMSD_{\text{inpcrd-restrt}}^{(i)}$$

0.1 mol/kcal *1.0 Å^{-1}*

Implications for PMMA Tacticity Control

$[Zn_2(BDC)_2DABCO]_n$

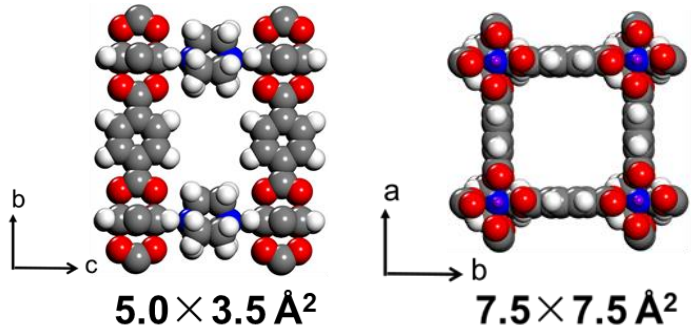

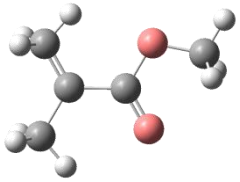

MMA monomer
size (5.9 × 4.1 Å²)

Example in $[Zn_2(BDC\text{-}2OCH_3)_2DABCO]_n$

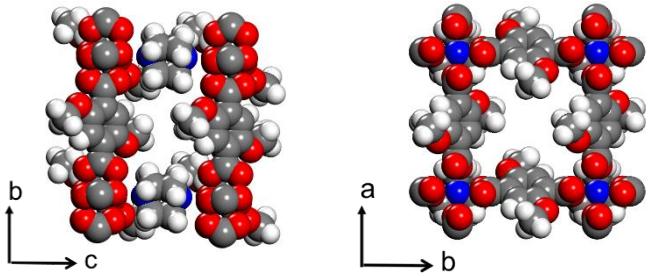

- In the planar structure, MMA monomers can approach favorably to radicals continuously along the 1D channels (c-axis)
- In the nonplanar structure, the expanded pore windows instead of narrow apertures can allow MMA monomers to be polymerized from 3D directions.
- The introduction of bulky substituents ($-CH_3$, $-NH_2$, $-OCH_3$) onto BDC linker may lead to less sterically isotactic conformation in polymerization.

Implications for PMMA Tacticity Control

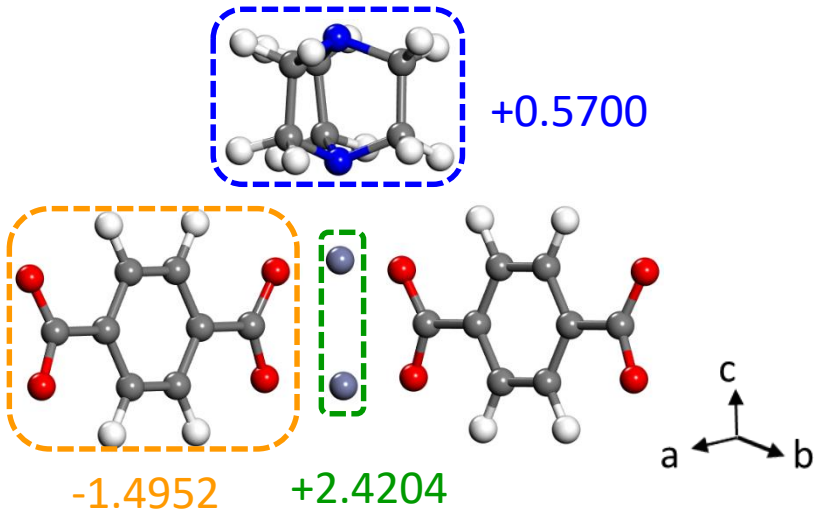

The introduction of polar substituents has a remarkable impact on charge distribution on BDC linker.

- *Example in mono-substituent with F, Cl and Br*

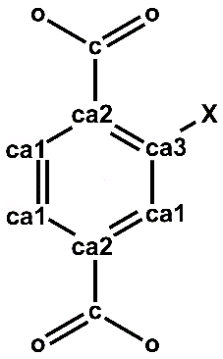

BDC-F		BDC-Cl		BDC-Br	
Atom type	**Mono-**	**Atom type**	**Mono-**	**Atom type**	**Mono-**
ca1	-0.1468	**ca1**	-0.0962	**ca1**	-0.0911
ca2	-0.1125	**ca2**	-0.0762	**ca2**	-0.0711
ha	0.1190	**ha**	0.1070	**ha**	0.0959
c	0.8748	**c**	0.8649	**c**	0.8684
o	-0.7694	**o**	-0.7673	**o**	-0.7690
f	-0.1945	**cl**	-0.1749	**br**	-0.1203
ca3	0.3357	**ca3**	0.1391	**ca3**	0.0921

➢ *The electrostatic interaction between the pore surface and PMMA will induce the preferred localization for polymerization by different substituents.*

Research Plan

Experimental results reveal that BDC linker with different substituents (BDC-X) can realize the controllable tacticity of product PMMA polymerization. However, the atomistic mechanism of PMMA tacticity control by different substituents on polymerization is still under discussion.

The First Step

- ✓ To prepare the force field (FF) parameters for MOFs channel by the introduction of different substituents

The Second Step

- ✓ Investigate radical polymerization process of PMMA in MOF channels
- ✓ To investigate the tacticity dependency of PMMA on the organic linkers composing the MOF by using MD simulation